THE ASTROPHYSICAL JOURNAL, 529:506–512, 2000 January 20

DETECTION TECHNIQUES OF MICROSECOND GAMMA-RAY BURSTS USING GROUND-BASED TELESCOPES

F. KRENNRICH,[1] S. LE BOHEC,[1] AND T. C. WEEKES[2]
Received 1999 May 7; accepted 1999 September 3

ABSTRACT

Gamma-ray observations above 200 MeV are conventionally made by satellite-based detectors. The EGRET detector on the *Compton Gamma Ray Observatory* has provided good sensitivity for the detection of bursts lasting for more than 200 ms. Theoretical predictions of high-energy gamma-ray bursts produced by quantum mechanical decay of primordial black holes (Hawking) suggest the emission of bursts on shorter timescales. The final stage of a primordial black hole results in a burst of gamma rays, peaking around 250 MeV and lasting for 1/10 of a microsecond or longer depending on particle physics. In this work we show that there is an observational window using ground-based imaging Cerenkov detectors to measure gamma-ray burst emission at energies $E > 200$ MeV. This technique, with a sensitivity for bursts lasting nanoseconds to several microseconds, is based on the detection of multiphoton-initiated air showers.

Subject headings: gamma rays: observations — instrumentation: detectors — radiation mechanisms: nonthermal

1. INTRODUCTION

The astrophysical band for the detection of high-energy gamma rays has been recently expanded to energies between hundreds of GeV (Weekes et al. 1989) up to beyond 10 TeV (Aharonian et al. 1997; Tanimori et al. 1998a; Krennrich et al. 1999) using the ground-based atmospheric Cerenkov imaging technique. The proposed coverage from 20 MeV–300 GeV with the future satellite-based *GLAST* detector (Gehrels & Michelson 1999) providing a large field of view is complemented by the proposals of ground-based detectors such as VERITAS (Weekes et al. 1999), HESS (Hofmann et al. 1997), and MAGIC (Barrio et al. 1998) with an energy threshold in the tens of GeV range. Ground-based Cerenkov imaging detectors provide large collection areas of the order of 10^5 m^2 and, hence, are well suited to the study of gamma-ray flare phenomena. This technique has already proven successful in the study of active galactic nucleus (AGN) flares on minute timescales (Gaidos et al. 1996) and is expected to improve in sensitivity by an order of magnitude with future detectors.

In this paper we explore the possibility of using imaging atmospheric Cerenkov telescopes to detect gamma-ray flare phenomena on shorter timescales of microseconds and with energies in the sub-GeV regime. Astrophysical phenomena producing extremely short bursts of gamma rays could be the signature of Hawking's prediction of gamma-ray burst radiation from the evaporation of primordial black holes (PBHs) (Hawking 1974). The lifetime of a black hole is proportional to the mass cubed. In the early universe PBHs of small mass may have formed (Hawking 1971; Carr 1976). PBHs created with initial masses slightly greater than $\approx 5 \times 10^{14}$ g would be evaporating now by the quantum gravitational Hawking mechanism. A PBH's existence ends in a dramatic explosion where the final stage of the evaporation is determined by particle physics at extremely high energies. Hagedorn (1970) suggested a particle physics model in which the number of species of particles increases exponentially with energy. In this scenario, a black hole loses its energy quickly when reaching a critical temperature. A burst of gamma rays as short as 10^{-7} s, with a total energy of 10^{34} ergs, would be the signature of such an event. However, the burst timescale and average photon energy depends on the particle physics model, with highly uncertain predictions at high energies. This has prompted searches over much larger timescales and energy scales ranging from 10^{-7} s at 250 MeV to seconds at 10 TeV, as suggested by the standard model of particle physics (Halzen et al. 1991). Cline & Hong (1992), using a mixture of a Hagedorn and QCD-like spectrum, suggested that these bursts occur on the millisecond timescale in the MeV range.

Classical gamma-ray bursts (GRBs) detected with the satellite experiment BATSE on *CGRO* show gamma-ray emission on surprisingly short timescales. GRB timescales in the millisecond range have been reported by Kouveliotou et al. (1994)—the detection of the so-called "Superbowl" burst (GRB 930131) has revealed temporal variations on timescales as short as 2 ms. In fact, evidence for sub-millisecond (200 μs) structures was found in the BATSE data of GRB 910305 (Bhat et al. 1992). EGRET, which was sensitive from 30 MeV to 30 GeV, because of an instrumental dead-time effect, was limited in sensitivity for short bursts to timescales above 200 ms.

A search for microsecond scale bursts using EGRET has been made by looking for multiple–gamma-ray events arriving almost simultaneously (within a single spark chamber gate, i.e., 600 ns); it produced only an upper limit of 5×10^{-2} yr^{-1} pc^{-3} (Fichtel et al. 1994). Searches by Cline et al. (1997) using archival data from the BATSE experiment found some events on millisecond timescales, but it was not possible to prove that they were not just classical gamma-ray bursters. Also in an early experiment, first-generation ground-based atmospheric Cerenkov detectors were used to search on the shortest timescales predicted (10^{-7} s), giving an upper limit of 4×10^{-2} yr^{-1} pc^{-3} (Porter & Weekes 1978). The possibility of using atmospheric Cerenkov imaging telescopes to detect wave front events was considered elsewhere (Connaughton, 1996); for a

[1] Department of Physics and Astronomy, Iowa State University, Ames, IA 50011-3160.
[2] Fred Lawrence Whipple Observatory, Harvard-Smithsonian CfA, P.O. Box 97, Amado, AZ 85645-0097.

single telescope with a camera with a relatively small field of view, it was shown to be difficult to recognize the bursts and distinguish them from background cosmic-ray events.

The technique described here can be used to search for microsecond gamma-ray emission in the sub-GeV regime with a more sensitive ground-based instrument. The proposed detection technique will clearly identify these events. A short burst can be approximated as a thin plane wave front of gamma-rays traveling through space (wave front event, hereafter), starting a multiphoton-initiated cascade when entering the Earth's atmosphere. Measuring the angular distribution of Cerenkov light from a short burst using an atmospheric Cerenkov imaging detector is a new approach to distinguish short bursts from background by cosmic rays. Previous efforts (Porter & Weekes 1978) used nonimaging Cerenkov detectors, and the suppression of cosmic rays was achieved by simultaneous recording by two telescopes separated at a distance of 400 km. Imaging enables the identification of a gamma-ray wave front event in a single telescope and the measurement of its arrival direction. With some modifications (§ 4), future ground-based gamma-ray detectors using arrays of imaging telescopes, e.g., VERITAS (Weekes et al. 1999) and HESS (Hofmann et al. 1997), would be ideally suited for exploring this observational window of microsecond bursts.

In § 2 we describe the phenomenology of the wave front events and how they differ from single-particle–initiated air showers. In § 3, using Monte Carlo simulations, we describe an analysis technique including timing characteristics to separate wave front events from background arising from cosmic-ray showers. We also discuss the design considerations (§ 4) for the implementation in imaging Cerenkov telescopes. In § 5, an estimate of flux sensitivity and the energy range of the existing Whipple Observatory 10 m instrument are shown.

2. PHENOMENOLOGY OF MULTIPHOTON-INITIATED SHOWERS

The technique proposed here builds upon the atmospheric Cerenkov imaging technique that has been pivotal in establishing the field of TeV gamma-ray astrophysics (for review, see Ong 1998). The technique provides the highest sensitivity for detecting gamma-ray sources above 200 GeV. In this technique, Cerenkov light from an electromagnetic atmospheric cascade is focused onto a camera of fast photomultiplier tubes. The images are analyzed to select gamma-ray events while rejecting over 99.7% of cosmic-ray background events. This has led to the discovery of TeV gamma rays from the Crab Nebula (Weekes et al. 1989), PSR 1706−44 (Kifune et al. 1995), Vela (Yoshikoshi et al. 1997), and SN 1006 (Tanimori et al. 1998b) and from three AGNs: Mrk 421 (Punch et al. 1992), Mrk 501 (Quinn et al. 1996), and 1ES 2344+514 (Catanese et al. 1998). Atmospheric Cerenkov telescopes have a high collection area ($\sim$50,000 m^2 for a single 250 GeV gamma ray) making them uniquely sensitive to short timescale phenomena.

Cerenkov light from a plane wave front of multiple $E > 200$ MeV gamma rays can be detected with ground-based optical telescopes. A low-energy multiphoton-initiated cascade differs significantly from a single-particle–initiated cascade, e.g., a TeV photon- or proton-induced shower. Individual low-energy gamma rays, when reaching the upper atmosphere, will typically generate one or a few (depending on energy) generations of electrons and positrons (collectively called electrons hereafter) by pair production and subsequent bremsstrahlung. The electrons, before falling below the critical energy, radiate Cerenkov light (6000 photons per electron for one radiation length), which can be collected by an optical reflector at ground level. The average number of Cerenkov photons associated with a single sub-GeV gamma ray is small, and, therefore, its Cerenkov flash is too faint to be detectable at ground level. However, a large number of gamma rays arriving within a short time can produce a Cerenkov signal strong enough to be detectable by an atmospheric Cerenkov telescope.

Previous efforts to detect wave front events were based on the fact that multiphoton-initiated showers have a large lateral extent. They can be detected by using relatively simple nonimaging atmospheric Cerenkov telescopes (Porter & Weekes 1978). For logistical and cost reasons it is difficult to operate two telescopes at a distance several hundred miles apart, solely dedicated to a search for bursts. On the contrary, existing imaging telescopes or future arrays of imaging telescopes can be used in parallel with standard TeV gamma-ray observations to search for wave front events from microsecond bursts. These instruments also provide a significant improvement to previous efforts: the imaging capability provides clear recognition of the wave front events from the measurement of the angular Cerenkov light distribution in the focal plane combined with the Cerenkov pulse width.

There are three unique characteristics of the Cerenkov light image produced by a wave front event:

1. The first is the very large extent of the wave front, which means it can be detected simultaneously by telescopes over vast distances. The images in all telescopes in an array (for example, the VERITAS array) should be identical, regardless of their distance. This is different from single-particle–initiated shower images that are detectable over a limited area on the ground and, if detected, show a parallactic displacement between telescopes.

2. The second characteristic is the time profile of the Cerenkov pulse that can range from $\approx$100 ns to microseconds—and thus is quite different from Cerenkov flashes of conventional air showers showing durations of 5–30 ns. The Cerenkov light time profile of relatively long (microsecond) bursts is dominated by the intrinsic width of the burst itself. However, the time profile of a wave front event is also determined by the geometry of the multiphoton-initiated cascade: the detection is based on collecting Cerenkov photons that have been emitted by secondary electrons of the cascades initiated by gamma-ray primaries with a large range of impact points. Cerenkov photons can be collected up to several hundred meters distance from the extrapolated impact point of the primary at ground level. The intrinsic differences in time of flight between Cerenkov photons from different primary particle impact points cause multiphoton-initiated showers to have a minimum width of $\approx$40 ns (see § 3.3), assuming the time profile of the gamma rays is a delta function. The time structure of the images shows a concentric symmetry: the closer to the center, the earlier the pulse.

3. The third characteristic, which is hinted at by Figure 1, but is not entirely obvious, is that the images in the camera plane from a wave front event are circular. They also will provide information about the arrival direction of the wave

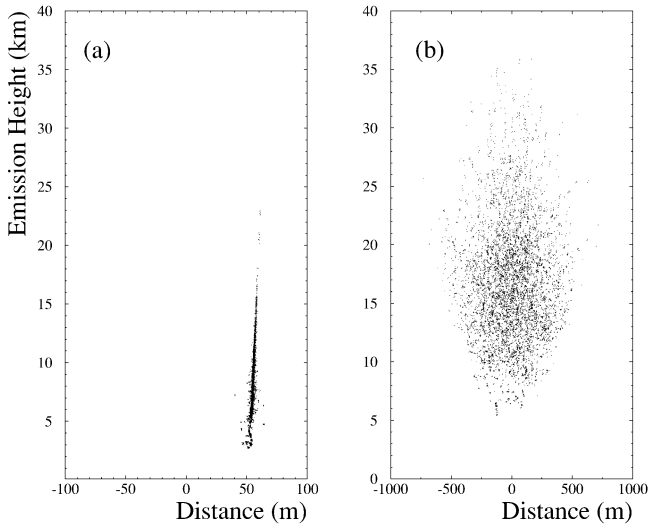

FIG. 1.—(*a*) Longitudinal and lateral distribution of the electromagnetic component of a single gamma-ray–initiated shower of 1 TeV, traced by the Cerenkov light, is shown. The dots indicate the origin of emission of individual Cerenkov photons that are detected with a Whipple-type telescope, located at an elevation of 2306 m and at *x*-coordinate zero. (*b*) We show the corresponding distribution for a multigamma-ray–initiated shower (note that lateral scale is a factor of 10 larger). The single 1 TeV gamma ray produces a narrowband Cerenkov photon distribution in the atmosphere. It can be detected up to a distance of 150 m from the shower core. For the multigamma-ray–initiated shower, Cerenkov photons that originate up to 600 m away in the lateral scale can still contribute to the Cerenkov flash detected in a telescope.

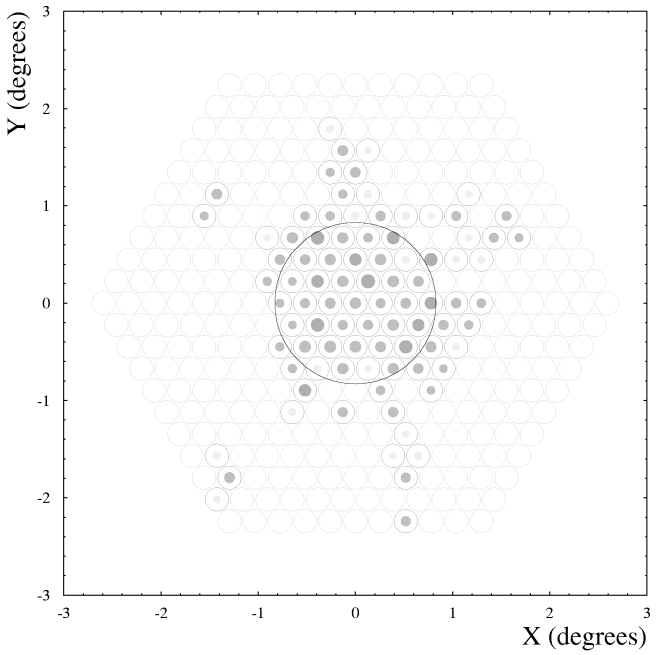

FIG. 2.—Simulated image of a burst of 300 MeV gamma rays (2.4×10^{-8} ergs cm^{-2}) arriving within 100 ns, as it would be seen with the Whipple Observatory 10 m telescope. The area and the gray scale of the filled circles indicate the relative light content in each pixel (maximum of 35 photoelectons per pixel in this event). Night-sky noise fluctuations for a 100 ns integration time are included. The image has been processed using the standard image-cleaning procedure (Reynolds et al. 1993). The circle indicates the angular extension and the shape of the image. The center of the circle coincides with the arrival direction of the burst to within 0°.1.

front: the displacement of the image centroid from the optic axis of the telescope measures the arrival direction of the burst.

Figure 2 shows the simulated image (see § 3.1) of a Cerenkov flash from a 300 MeV gamma-ray burst (pulse width of 100 ns with 0.5 gamma rays m^{-2}; fluence = 2.4×10^{-8} ergs cm^{-2}) in the focal plane of the Whipple Observatory 10 m telescope. The background from night-sky fluctuations for a 100 ns exposure has been included and a standard image-cleaning procedure (Reynolds et al. 1993) applied. The light distribution in the image center is relatively flat and smooth. The flatness of the light distribution arises from a uniform lateral density distribution of electrons. Shower fluctuations have very little effect on the Cerenkov light distribution because of the huge number of showers contributing to the Cerenkov flash. This results in a smooth light distribution with mainly statistical variations due to the night-sky background and instrumental noise.

The Cerenkov light angular distribution is determined by the Cerenkov angle at a given height (0°.4 at 15 km height) and the multiple scattering angle of the electrons in the cascade. The convolution of both effects leads to images that show a prominent plateau with a radial extension of $\approx 0°.3$ with a "halo" extending further with a scale of $\approx 2°$ FWHM. These image shapes clearly differ from single gamma-ray or cosmic-ray–initiated Cerenkov images (Hillas 1996) and provide an important constraint for classifying these short bursts. Together, with the timing information of the Cerenkov pulse shape, imaging can be used to reject background events from cosmic rays.

Because we are describing a burst detection technique, fluence and sensitive area are used to describe the detector properties and are defined as follows:

1. *Fluence.*—A detector is triggered whenever the number of gamma rays during an integration time bin of some duration exceeds a threshold. In the following, we use the term fluence, the total energy S received from a given burst in units of ergs cm^{-2} over the full duration of the burst. Since we are not trying to resolve individual photons during the burst, such an integral measure is sufficient.

2. *Sensitive area.*—Cerenkov photons emitted by an electron at 20 km atmospheric height are most likely spread over an area of 500 m in radius. However, a few photons, emitted from electrons with large multiple scattering angles, reach up to 800 m from the impact point of the primary gamma ray. This results in a large sensitive area (2×10^6 m^2) over which individual gamma rays make a contribution to the total amount of light of a Cerenkov flash. The efficiency for a single sub-GeV gamma ray triggering a reasonably sized atmospheric Cerenkov imaging telescope (<20 m reflector diameter) is essentially zero. For a 300 MeV gamma ray, the efficiency for contributing a single photoelectron in the photomultiplier camera of the Whipple Observatory 10 m telescope reaches a maximum of approximately 1%. The sensitive area is the area for which an individual low-energy shower makes a significant contribution to the Cerenkov light flash.

3. SIMULATIONS

We have carried out Monte Carlo simulations to characterize the signatures of multiphoton-initiated cascades. The Monte Carlo code ISUSIM (Mohanty et al. 1998) was used, which includes the detector model of the Whipple Observa-

tory 10 m telescope equipped with a 4°.8 field-of-view, 331 photomultiplier camera (Quinn et al. 1999). The underlying goal was to achieve good background suppression while maintaining maximum detection efficiency.

A microsecond burst consists of multiple primary gamma rays producing independent cascades. We have generated 10^8 individual gamma rays randomly spread out over a range of impact radius 0–1000 m to study the properties of bursts. The Cerenkov photons that hit the mirror and are reflected into the focal plane detector have been superimposed. In order to trigger on a wave front event, the number of photoelectrons created in several photomultipliers used for forming a coincidence has to significantly exceed the number of photoelectrons initiated by fluctuations from the night-sky background. Therefore, a minimum number of gamma rays per square meter (Cerenkov photon yield $\sim$ number of primary gamma rays) is required to detect a signal in the photomultiplier camera (for trigger specifications, see § 4). The fluence required for the detection of a wave front event of given gamma-ray energies is proportional to the number of incoming gamma rays m^{-2} during the time of the burst, ultimately determining the number of Cerenkov photons arriving at the detector.

3.1. *Image Characteristics*

The technique of recording the Cerenkov images of single-particle–induced showers has proved to be effective in distinguishing gamma-ray–induced showers from the more numerous background images from cosmic rays. The usefulness of imaging to identify wave front events is addressed in this section.

Figure 2 shows the Cerenkov light image from a simulated wave front event (300 MeV gamma rays traveling parallel to the optic axis) in the 331 phototube camera of the Whipple Observatory 10 m telescope. The area and the gray scale of the filled circles indicates the number of photoelectrons detected in each pixel. The fluence of the event in Figure 2 is 2.4×10^{-8} ergs cm^{-2} (0.5 gamma rays m^{-2} at 300 MeV). Figure 3 shows the image of a wave front event arriving 1°.13 off-axis, and it can be seen that the image is off-set by $\approx$1°.1 from the center of the camera. The image center can be used to measure the arrival direction of the burst. In both cases the light distribution shows a circular image. In the case of the image in Figure 3, the fluence is 2 times higher than in Figure 2 and a smoothly decreasing "halo" can be seen. The light beyond the central plateau (0°.3 in radius) is caused mainly by the multiple scattering of relatively low energy electrons. This halo is not easily recognizable in Figure 2 (where the burst has a lower fluence) because the amount of light is comparable to the noise fluctuations from the night-sky background.

The structure of the image can be described by its circular shape and its characteristic radius. The image shape is described here using a combination of the parameters, width and length (Hillas 1985). The eccentricity of an image, characterizing its circular shape, is defined by: eccentricity = $(1 - \text{width}^2/\text{length}^2)^{1/2}$. A perfectly circular image would have an eccentricity equal to zero. The radial extent of the images is described by radius, defined by: radius = (width + length)/2. The radius and eccentricity distribution for wave front events (individual gamma rays of 200 MeV–5 GeV sampled from a power-law distribution with a differential spectral index of -2.5) are shown in Figures 4*b* and 5*a*, respectively. The radius of the images is well defined and substantially bigger than for most cosmic-ray showers. A selection of images with radius > 0°.70 would reject most cosmic-ray images. The eccentricity distribution peaks at 0.2 (Fig. 5*a*), which corresponds to mostly

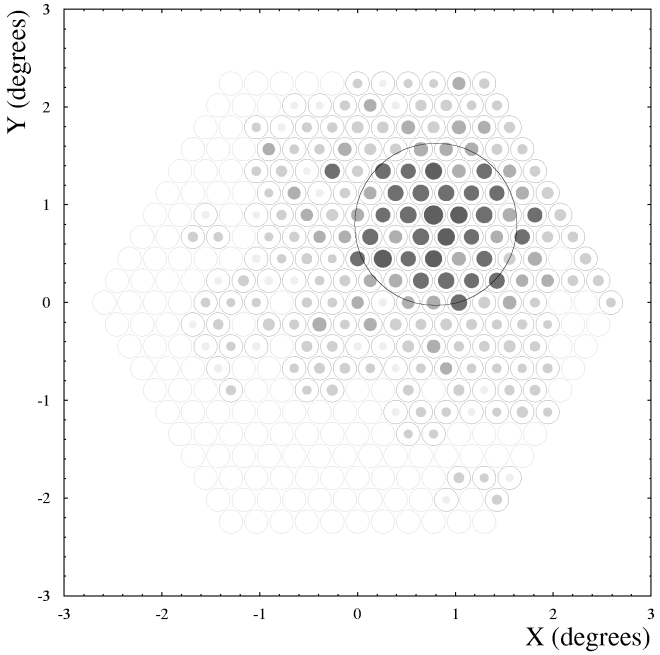

FIG. 3.—Simulated image of a burst of 300 MeV gamma rays lasting for 100 ns with a photon density of (fluence = 4.8×10^{-8} ergs cm^{-2}). The arrival direction was offset by 1°.13 from the optic axis of the telescope. Image processing using the standard image-cleaning procedure (Reynolds et al. 1993) has been applied. The circle indicates the plateau and the drop in the light density of the image where its center coincides with the arrival direction of the burst. The smooth "halo" surrounding the central image is the other characteristic feature of a burst when its light content is significantly above the night-sky noise.

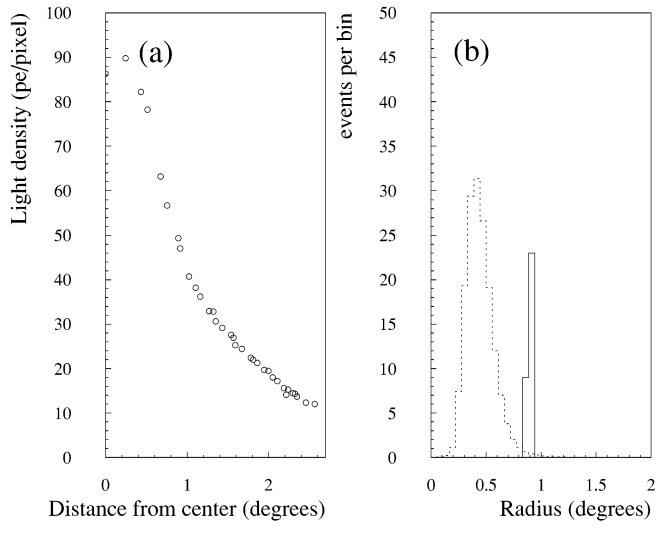

FIG. 4.—(*a*) Average radial light profile (light density vs. radial distance from image center) of wave front events is shown. (*b*) The estimated *Radius* of simulated wave front events (*solid line*) is compared with the radius of detected cosmic-ray background events (*dashed line*). Only cosmic-ray events with the same or larger light content (size) in the image as for the simulated wave front events are accepted. The average *Radius* of the images from 500 MeV bursts is approximately 0°.8, which corresponds to the half-width in the radial profile.

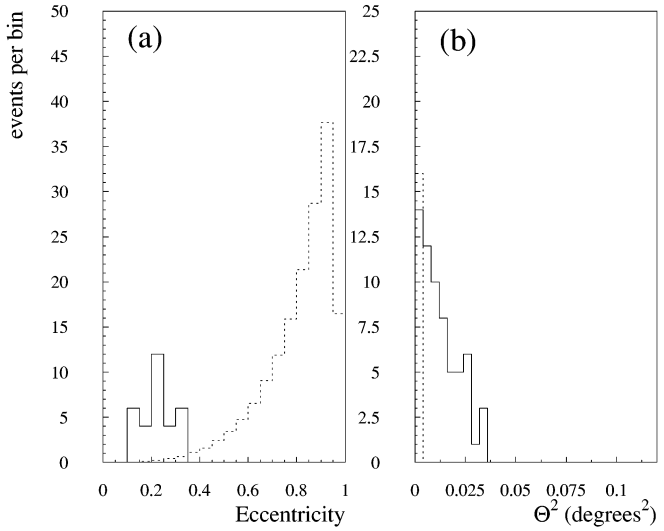

FIG. 5.—(*a*) *Eccentricity* $[(1 - \text{Width}^2/\text{Length}^2)^{1/2}]$ of images from wave front events are shown. The distribution for wave front events peaks at 0.2, as expected for almost circular images. The dotted curve represents cosmic-ray showers recorded with the Whipple Observatory 10 m telescope. (*b*) The square of the difference between the reconstructed arrival direction from the true arrival direction (Θ^2) of wave front events is plotted. The angular resolution is 0°.12 for a burst close to the detection threshold (*solid line*) and becomes 0°.06 for bursts with 4 times higher fluence values (*dotted line*). Background images from cosmic rays with isotropic arrival directions would show a flat distribution in this representation.

circular images, establishing their circular shape. Given the radius and eccentricity distribution of recorded cosmic-ray showers (dotted line in Figs. 4*b* and 5*a*), a strong background suppression can be achieved in the search for multiphoton-initiated cascades.

An additional feature that can be used is the relatively smooth light distribution, which is very different from most cosmic-ray shower images. The images from wave front events reflect the fact that many showers contribute to an image: their light distribution is extremely smooth. The smoothness of an image can be quantified, e.g., by calculating the rms of the light content of all pixels.

3.2. *Angular Resolution*

The image center position provides an estimate of the true arrival direction of a wave front event. The angle Θ is the difference between the reconstructed and the true arrival direction in degrees. Figure 5*b* shows the Θ^2 distribution of simulated bursts with each burst containing energies 0.2–5 GeV sampled from power law of $E^{-2.5}$. The reconstruction accuracy also depends on the total amount of light collected and therefore the fluence of the burst. The angular resolution σ_Θ is defined here so that 72% of the image centers would fall within a radius of σ_Θ. The resolution for a burst with a fluence of 1.5×10^{-8} ergs cm^{-2} is $\sigma_\Theta = 0°.12$. However, for a burst with a fluence of 6.0×10^{-8} ergs cm^{-2} the resolution is $\sigma_\Theta = 0°.06$ and improves approximately with the square root of the fluence.

3.3. *Timing Characteristics*

Images of wave front events have a characteristic shape, but even so, image analysis might not remove the background from cosmic-ray–induced showers completely. The pulse shape of the Cerenkov light pulse provides an additional signature to identify and distinguish multiphoton-initiated cascades from single-particle–initiated air showers. Pulse shapes from cosmic-ray air showers are typically a few nanoseconds wide. Multiparticle-initiated showers from bursts show a minimum timescale of at least 40 ns.

We have used the Whipple Observatory 10 m telescope to record pulse shapes of cosmic-ray–induced air showers utilizing a four-channel digital oscilloscope (Hewlett-Packard 54540A) with a 500 MHz sampling time. Four channels were used to record pulses from phototubes that were spread out over an area of 0°.5 × 0°.5 in the focal plane. The trigger requires all four channels to ensure that the system would only record pulses from fairly extended images, similar to multiphoton-initiated events. Smaller images can be distinguished by imaging, e.g., by measuring their *Radius* and *Eccentricity*. The oscilloscope readout was initiated whenever four channels exceeded a threshold of 30 mV with a time overlap of at least 10 ns. The length of each record was chosen to be 2 μs with a time resolution of 4 ns. The recording system, including the photomultiplier, cables, and amplifiers used, was sensitive to pulse widths ranging from 10 ns up to several hundred ns.

Figure 6*a* shows the pulse shape of a typical Cerenkov light flash recorded with the Whipple Observatory 10 m telescope. In comparison we show (Fig. 6*b*) the simulated pulse profiles from a multiphoton-initiated cascade from a 100 ns burst of 500 MeV gamma rays of two different pixels: in the center of the image (*solid line*) and a pixel 1° off-center (*dashed line*). The pulse profiles of the multiphoton-initiated cascade are broad and only slightly shifted with respect to each other. The fluence for the simulated wave front event is 1.1×10^{-7} ergs cm^{-2}, about 7 times higher than the sensitivity limit of the technique using the Whipple Observatory 10 m telescope. It is important to point out that our measurement gives a limit for the background expected for a

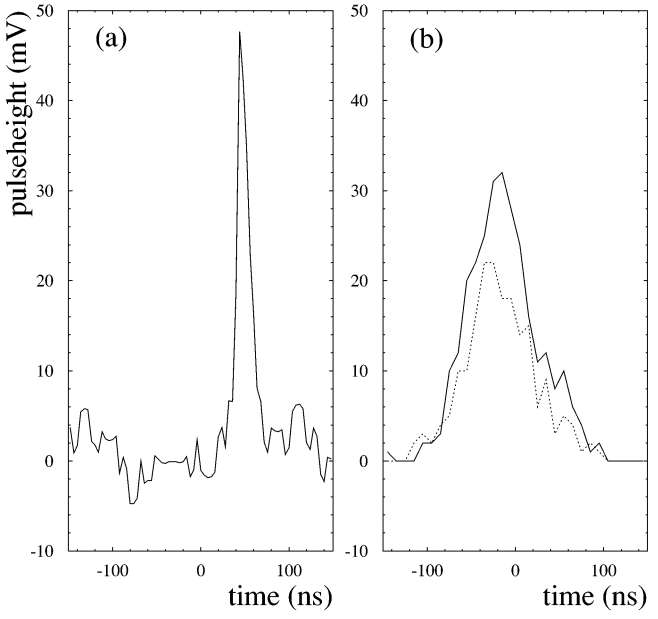

FIG. 6.—(*a*) Pulse shape for a cosmic-ray event recorded with the Whipple 10 m telescope is shown. The noise is the result of fluctuations from the night-sky background light. (*b*) The pulse profile of a simulated multiphoton-initiated cascade for two photomultipliers, one in the center of the image (*solid line*) and one by 1° off-center (*dotted line*), are shown. The burst timescale is 100 ns. Here the night-sky background noise is not included, but it would be comparable to the noise in Fig. 5*a*.

burst sensitivity 1.1×10^{-7} ergs cm^{-2}. Operating at a lower threshold might imply a higher background.

Figure 7 shows the distribution of pulse widths for a data sample consisting of 10,000 events taken during 6 hr of observation time. The longest pulse recorded shows a FWHM of 33 ns. It is important to notice, that the pulse widths presented here are broadened by 180 feet (54.864 m) of coax cable (RG-58). The intrinsic pulse width of Cerenkov pulses are somewhat shorter. This clearly indicates that pulse profiles provide excellent background discrimination of cosmic rays. Note, that even with this relatively simple setup, a sensitivity of 1.1×10^{-7} ergs cm^{-2} for bursts of 500 MeV gamma rays would be reached.

3.4. *Other Sources of Background*

A second background showing time profiles similar to those of multiphoton-initiated cascades could arise from fluorescence light of ultra–high-energy cosmic rays (UHECR) at $E > 10^{16}$ eV. Although rare, they could constitute a background of slow pulses. The recorded image of the event will help to reject fluorescence events: the image would appear as an extended band through the camera, as opposed to a circular flat image from a wave front of multiple gamma rays. The pulse profiles of fluorescence light depends on the impact parameter and the arrival direction of the UHECR-shower (Baltrusaitis et al. 1985). For the pixellation of the Whipple camera (0.°25), the pulse width of a UHECR-shower ranges from 70 to 350 ns for an impact parameter of 5 and 1 km, respectively. Fluorescence light events can be distinguished from wave front events by the average arrival time of photons (center of the pulse) in various pixels across the field of view. They differ according to the geometrical time-of-flight difference between the telescope and different parts of the shower. As a consequence, the pulses in different pixels of a fluorescence event should be substantially shifted with respect to each other along the shower axis, whereas the average arrival times of pulses from a wave front event have a small intrinsic time spread and a circular symmetric arrival time pattern. Therefore, it is expected that even with a single telescope, rare fluorescence events could be eliminated.

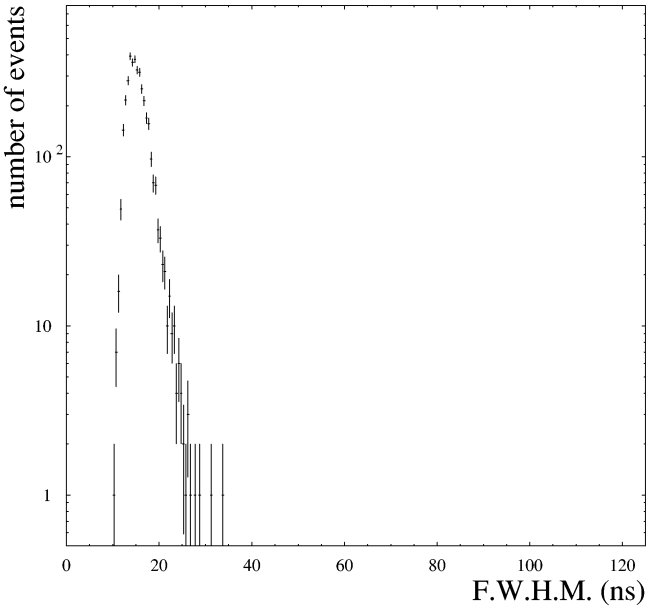

FIG. 7.—Pulse width distribution for events recorded with the Whipple 10 m telescope. The expected range for bursts from PBHs would be above 100 ns. The shortest possible pulse width from a multiphoton-initiated cascade that occurs as a result of arrival time differences between the subshowers is at about 40 ns.

Light flashes from meteors and lightning have to be considered as a potential source of background. The time constant of faint meteors is of order 10 ms or greater (Cook et al. 1980) and is not in the range of microsecond bursts. Lightning pulses are in the range of tens to hundreds of microseconds (P. Krider, private communication 1999).

4. TRIGGER CRITERIA

The properties of images from wave front events are vastly different than typical gamma-ray images, for which imaging Cerenkov telescopes are usually optimized. Images from TeV gamma-ray primaries exhibit a small angular spread requiring a trigger sensitive to an elliptical image extending over an area of $\approx 0.°15 \times 0.°30$ in the field of view. Thus Cerenkov telescopes often have a trigger requirement of a twofold (fourfold for high-resolution cameras) coincidence. The large angular extent of wave front images puts a very different requirement on the trigger geometry—covering a solid angle of $\approx 1.°5$ in diameter. The limiting factor in both cases is fluctuations from the night-sky background light. The signal-to-noise ratio needs to be optimized in order to achieve the highest sensitivity. In case of wave front events, the image is bright within the central 1.°5, the highest signal-to-noise ratio would be achieved by triggering on the total light covering the central 1.°5 of the image. A highfold coincidence over pixels could be used to trigger efficiently on wave front events helping to reduce the random triggers arising from the night-sky background light fluctuations. Using a pixellation of 0.°25 (see Fig. 2), a highfold coincidence of 40 pixels would provide a reasonable trigger condition.

Also, the timing characteristics of the trigger, providing a good sensitivity for wave front events, are different than for TeV gamma-ray observations. Single gamma-ray detection uses a typical coincidence time of 10 ns. Wave front event recording would be based on the integration timescale in the order of 100 ns up to a few microseconds depending on the putative astrophysical burst timescale. It is important to point out that in case of wave front detection an integration of the signal over the burst timescale is most efficient to increase the signal-to-noise ratio at the trigger level. To search for astrophysical phenomena whose emission timescale is uncertain, a trigger operating at several different timescales in parallel is necessary, similar to the technique used for the Fly's Eye detector (Baltrusaitis et al. 1985).

5. SENSITIVITY

The detection of bursts using the imaging technique as described in this paper involves two steps: triggering on the Cerenkov light flash associated by the multiphoton-initiated cascade and discriminating a wave front event from cosmic-ray showers. Both requirements impact the sensitivity at a given energy and burst timescale. The sensitivity for a Whipple type 10 m telescope equipped with a 4.°8 field-of-view camera with 331 pixels is estimated (see also Quinn et al. 1999).

The trigger threshold for the detection of short bursts is a function of the fluence of the burst, expressed in ergs cm^2. The fluence is the product of the energy of the incoming particles and the number of particles per unit area imping-

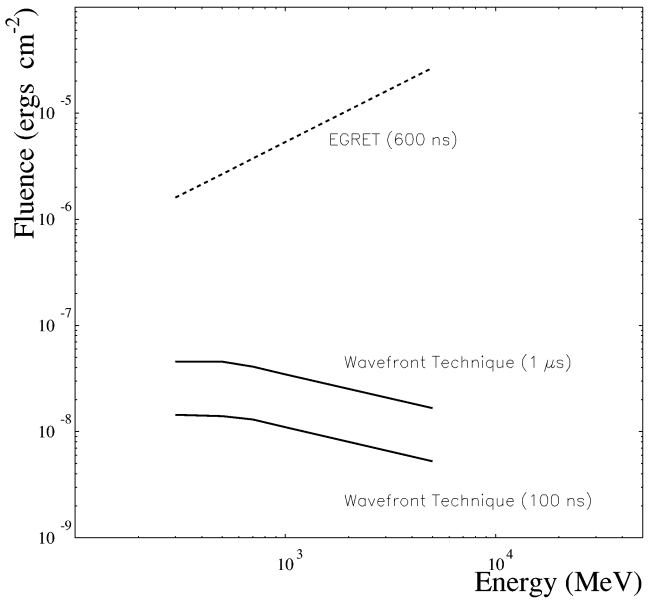

FIG. 8.—Fluence sensitivity for the wave front technique is shown as a function of energy. For comparison we also show the fluence sensitivity for EGRET, with a collection area of 0.15 m^2 in the given energy range. The detection of at least five gamma rays has been required. It can be seen that the wave front technique is about 2 orders of magnitude more sensitive than EGRET, which is mainly limited by its collection area.

ing on the upper atmosphere. In order to trigger on a wave front event we require 40 pixels to exceed the night-sky background fluctuations by 3 σ. This not only prevents triggering on night-sky background fluctuations, it also ensures a good image reconstruction. Figure 8 shows the fluence sensitivity as a function of energy for 100 ns and 1 μs burst timescale. For comparison to previous efforts we also show the sensitivity of the EGRET detector. EGRET has a sensitivity for bursts lasting for 600 ns where it records multiple events within one readout cycle. We have assumed here a collection area of 0.15 m^2 and a minimum of five gamma rays to be detected. Over the energy range of 300 MeV to 1 GeV the sensitivity of the wave front technique could exceed EGRET's sensitivity by a factor of 100–500 for 100 ns bursts.

The energy threshold for the detection of wave front events is limited to lower energies by the multiple scattering angle and by the Cerenkov threshold for radiation by electrons of 90 MeV at 20 km atmospheric height. This results in a natural barrier for the atmospheric Cerenkov technique. We have limited our simulations to energies between 200 MeV and 5 GeV.

6. SUMMARY

We have shown that sub-GeV gamma-ray bursts lasting for less than 100 ns to microseconds could be efficiently detected using a single ground-based imaging Cerenkov telescope. The technique described is based on previous attempts to detect multiphoton-initiated cascades from short bursts. However, we show for the first time that the angular Cerenkov light distribution together with the pulse shape can be used to advantage to search for short bursts with a single-imaging telescope.

Measurements of Cerenkov pulse shapes of cosmic-ray–induced showers indicates that pulse shapes from multiphoton-initiated cascades are well separated from background showers. A search for microsecond bursts would use this criterion as a first filter. If events with long pulse durations were found, image analysis could verify if those events are consistent with the very distinct image shapes of a multiphoton-initiated cascade. The image also contains valuable information about the arrival direction with an angular resolution of 0°.06–0°.12, depending on the fluence. The fluence sensitivity of the Whipple telescope with a microsecond trigger exceeds EGRET's sensitivity by more than 2 orders of magnitude.

In addition, arrays of telescope could be used to improve this technique further. In contrast to air showers, wave front events would appear identical in the field of view of arrays of telescopes with a typical spacing of $\approx$100 m. Single-particle–initiated air showers show a parallactic displacement because of the different distances to the shower core. In view of several proposed next generation detectors (VERITAS, HESS; for overview, see Krennrich 1999), the implementation of this technique in telescope arrays could provide the highest fluence sensitivity of any existing gamma-ray detector for microsecond bursts at sub-GeV to several-GeV energies.

This research is supported by grants from the US Department of Energy.

REFERENCES

Aharonian, F. A., et al. 1997, A&A, 327, L5
Baltrusaitis, R. M., et al. 1985, Nucl. Instrum. Methods Phys. Res., A240, 410
Barrio, J. A., et al. 1998, The MAGIC Proposal, MPI-PhE/98-5 (Munich: MPI)
Bhat, P. N., et al. 1992, Nature, 359, 217
Carr, B. C. 1976, ApJ, 206, 8
Catanese, M., et al. 1998, ApJ, 501, 616
Cline, D. B., & Hong, W. 1992, ApJ, 401, L57
Cline, D. B., Sanders, D. A., & Hong, W. 1997, ApJ, 486, 169
Connaughton, V. 1996, Ph.D. thesis, Univ. College, Dublin
Cook, A. F., Weekes, T. C., Williams, J. T., & O'Mongain, E. 1980, MNRAS, 193, 645
Fichtel, C., et al. 1994, ApJ, 434, 557
Gaidos, J. A., et al. 1996, Nature, 383, 319
Gehrels, N., & Michelson, P. 1999, Astropart. Phys., 11, 277
Hagedorn, R. 1970, A&A, 5, 184
Halzen, F., Zas, E., MacGibbon, J. H., & Weekes, T. C. 1991, Nature, 353, 807
Hawking, S. W. 1971, MNRAS, 152, 75
———. 1974, Nature, 248, 31
Hillas, A. M. 1985, Proc. 19th Internat. Cosmic Ray Conf. (La Jolla), 3, 445
———. 1996, Space Sci. Rev., 75(1–2), 17
Hofmann, W., et al. 1997, in Proc. Towards a Major Atmospheric Cerenkov Detector–V, ed. O. C. de Jager (Potchefstroom: Space Research Unit, Univ. of South Africa), 405
Kifune, T., et al. 1995, ApJ, 438, L91
Kouveliotou, C., et al. 1994, ApJ, 422, L59
Krennrich, F. 1999, Astropart. Phys., 11, 235
Krennrich, F., et al. 1999, ApJ, 511, 149
Mohanty, G., et al. 1998, Astropart. Phys., 9, 15
Ong, R. A. 1998, Phys. Rep., 305, 93
Porter, N. A., & Weekes, T. C. 1978, MNRAS, 183, 205
Punch, M., et al. 1992, Nature, 358, 477
Quinn, J., et al. 1996, ApJ, 456, L83
———. 1999, ApJ, 518, 693
Reynolds, P. T., et al. 1993, ApJ, 404, 206
Tanimori, T., et al. 1998a, ApJ, 492, L33
———. 1998b, ApJ, 497, L25
Weekes, T. C., et al. 1989, ApJ, 342, 379
———. 1999, VERITAS Proposal (to the Department of Energy)
Yoshikoshi, T., et al. 1997, ApJ, 487, L65